Proton-Proton Correlations in $^{40}Ar + ^{197}Au$ Reactions and the Role of the Two-Particle Phase Space

G. J. Kunde,[1] J. Pochodzalla,[1,2] E. Berdermann,[1] B. Berthier,[3] C. Cerruti,[4] C. K. Gelbke,[5] J. Hubele,[1] P. Kreutz,[2] S. Leray,[4] R. Lucas,[3] U. Lynen,[1] U. Milkau,[1] C. Ngô,[4] C. H. Pinkenburg,[2] G. Raciti,[6] H. Sann,[1] and W. Trautmann[1]

[1]*Gesellschaft für Schwerionenforschung, D-6100 Darmstadt, Germany*
[2]*Institut für Kernphysik, Universität Frankfurt, D-6000 Frankfurt, Germany*
[3]*Departement de Physique Nucléaire, Centre d'Etudes Nucléaires de Saclay, F-91191 Gif-sur-Yvette CEDEX, France*
[4]*Laboratoire National Saturne, Centre d'Etudes Nucléaires de Saclay, F-91191 Gif-sur-Yvette CEDEX, France*
[5]*National Superconducting Cyclotron Laboratory, Michigan State University, East Lansing, Michigan 48824*
[6]*Department of Physics, University of Catania, I-95129 Catania, Italy*

(Received 6 October 1992)

Proton-proton correlations at small relative momenta were measured for $^{40}Ar + ^{197}Au$ reactions at $E/A = 200$ MeV. Comparing the correlation functions to predictions based on single-particle phase space distributions from microscopic Boltzmann-Uehling-Uhlenbeck and quantum-molecular-dynamics (QMD) simulations, no satisfactory agreement could be established. Calculations utilizing two-particle emission probabilities predicted by the QMD model differ significantly from the single-particle calculations and are much closer to the experimental observations at $E/A = 200$ MeV, potentially signaling the importance of the two-particle density for the proton-proton correlation function.

PACS numbers: 25.70.Pq, 24.60.Ky

To explore the space-time characteristics of the emission zone pair correlations between coincident protons have been studied intensively over the last years [1–8]. In most of these studies—and in particular in those at higher energies [2,4,8]—the interpretation relies on the assumption of a spherical source. However, two-particle correlations are also influenced by lifetime effects [1,7] and the reaction dynamics [9,10]. Additional complications might result from fluctuations of the Coulomb field of the residual nuclear system [11], polarization phenomena [12,13], and theoretical uncertainties of the interaction between the two nucleons in a nuclear medium. Finally, all two-particle correlation studies face the problem that an unambiguous relation between the observed correlation function (CF) and the source distribution does not exist. Nonetheless, each given model makes definite predictions about the source distribution and, hence, the CF.

Recently, significant progress has been achieved by Pratt and Bauer who computed proton-proton correlations on the basis of microscopic simulations of nucleus-nucleus collisions [14,15]. Using single-particle emission probabilities predicted by the Boltzmann-Uehling-Uhlenbeck (BUU) transport equation, these calculations provided a good description of CFs measured at intermediate beam energies, $E/A < 100$ MeV. In the present Letter, we report CFs of protons emitted in collisions between ^{40}Ar and ^{197}Au at $E/A = 200$ MeV. Calculations which are based on *single*-particle distributions predicted by microscopic models show no satisfactory agreement with the measured CFs. On the other hand, simulations using *two*-particle emission probabilities provided by the quantum-molecular-dynamics (QMD) model allow a reasonable description of these data.

The experiment was performed at the Laboratoire National SATURNE in Saclay. A gold target of 87

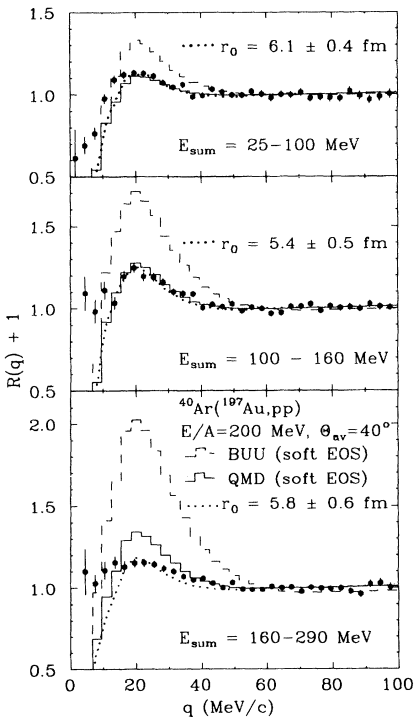

FIG. 1. Two-proton correlation functions measured for ^{40}Ar induced reactions on ^{197}Au at $E/A = 200$ MeV and different constraints on the sum energy E_{sum}. The lines are discussed in the text.

mg/cm^2 areal density was irradiated by ^{40}Ar ions with an incident energy of $E/A=200$ MeV. Light particles were detected by a closely packed 8×8 array of 64 ΔE-E telescopes, each consisting of a 300 μm thick silicon detector and a 6 cm thick CsI(Tl) crystal read out via a photodiode. Each telescope had an active area of 25×25 mm^2. The center of the hodoscope was positioned at a laboratory angle of $\Theta_{av}=40°$ at a distance of about 1 m from the target. The energy calibration of individual telescopes is accurate to within 3%. In the off-line analysis, lower and upper limits of 10 and 145 MeV, respectively, were applied by software on the kinetic energy of the protons.

We define the experimental correlation function $R(q)$ in terms of the number of true coincidences $N(q)$ for a given momentum of relative motion, q, and a background $M(q)$ obtained by mixing particles from different coincidence events:

$$R(q)+1=kN(q)/M(q)\,. \tag{1}$$

For each constraint on the summed kinetic energy $E_{sum}=E_1+E_2$ and for all theoretical CFs discussed below the normalization constant k is chosen such that $\langle R(q)\rangle=0$ in the interval $50\le q\le80$ MeV/c.

Correlation functions for different intervals of E_{sum} are displayed in Fig. 1. Unlike in previous studies at lower energies for the same reaction [6] no significant dependence on E_{sum} is observed. In order to quantify the experimental observations, we parametrize the data in terms of theoretical CFs assuming spherical Gaussian-shaped sources of density $\rho(r)\propto e^{-r^2/r_0^2}$ and negligible lifetime [1] (see dotted lines in Fig. 1). It is interesting to note that the apparent source radii r_0 follow the kinetic energy systematics of Ref. [12].

For a summary of our observation we introduce the mean CF $\langle R(q)+1\rangle_{15-27}$ in the region of the maximum $15\le q\le27$ MeV/c. The dots in Fig. 2 show these values for the ^{40}Ar+^{197}Au reaction at $E/A=200$ MeV (upper panel) and at $E/A=60$ MeV (lower panel [6]) as a function of E_{sum}. In the following we will compare this quantity to predictions based on microscopic simulations. In these calculations the probability to create two protons with momenta $\mathbf{p}_1$ and $\mathbf{p}_2$ such that both protons fall within the acceptance of the experimental apparatus will be denoted as $\Pi_2(\mathbf{p}_1,\mathbf{p}_2,\mathbf{r}_1,\mathbf{r}_2)$. Here, $\mathbf{r}_1$ and $\mathbf{r}_2$ are the positions of these protons at the time of emission of the second proton. We assume that the final-state interaction (FSI) is turned on once the second proton is emitted and that the particles propagate freely after their emission. On account of the lifetime of ^{2}He, the relative distance at the final time step is used for calculating the correlation for protons contained in diprotons (see below). Then, similar to the treatment in Ref. [15], $R(q)$ can be written as

$$R(q)+1=C_{FSI}(q)C_{dyn}(q)C_{\Delta}(q)\,. \tag{2}$$

The CF due to the FSI is given by

$$C_{FSI}(q)=\frac{\int d\mathbf{b}\,d\mathbf{p}_1\,d\mathbf{p}_2\,d\mathbf{r}_1\,d\mathbf{r}_2\,\Pi_2(\mathbf{p}_1,\mathbf{p}_2,\mathbf{r}_1,\mathbf{r}_2)\hat{\mathcal{C}}(\mathbf{q},\mathbf{r}_1-\mathbf{r}_2)\Theta_{\Delta}(q)}{\int d\mathbf{b}\,d\mathbf{p}_1\,d\mathbf{p}_2\,d\mathbf{r}_1\,d\mathbf{r}_2\,\Pi_2(\mathbf{p}_1,\mathbf{p}_2,\mathbf{r}_1,\mathbf{r}_2)\Theta_{\Delta}(q)}\,. \tag{3}$$

Here, $\hat{\mathcal{C}}(\mathbf{q},\mathbf{r}_1-\mathbf{r}_2)$ is defined as the correlation due to the FSI [1] and $\mathbf{b}$ is the impact parameter vector. The difference between the two-particle and single-particle emission probabilities *in momentum space* is reflected in the dynamical CF

$$C_{dyn}(q)=\frac{\int d\mathbf{b}\,d\mathbf{p}_1\,d\mathbf{p}_2\,d\mathbf{r}_1\,d\mathbf{r}_2\,\Pi_2(\mathbf{p}_1,\mathbf{p}_2,\mathbf{r}_1,\mathbf{r}_2)\Theta_{\Delta}(q)}{\int d\mathbf{p}_1\,d\mathbf{p}_2'\,\Pi_1(\mathbf{p}_2')\Pi_1(\mathbf{p}_1)\Theta_{\Delta}(q)}\,. \tag{4}$$

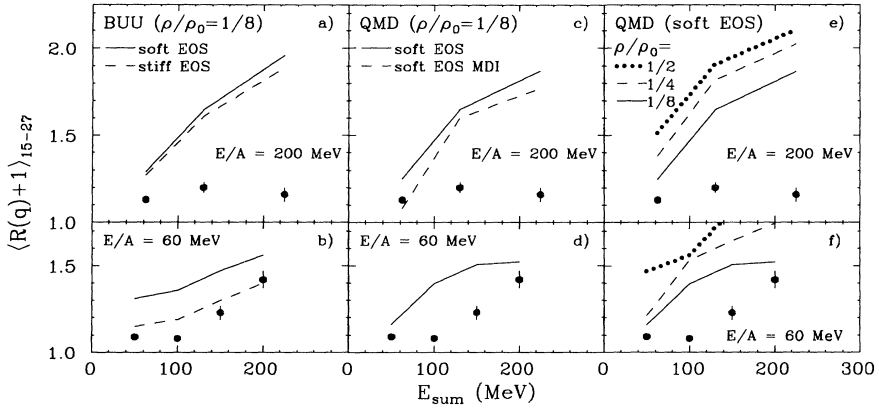

FIG. 2. Average height $\langle R(q)+1\rangle_{15-27}$ of the two-proton correlation functions as a function of the sum energy E_{sum} for ^{40}Ar+^{197}Au reactions at $E/A=60$ MeV (lower panels [6]) and $E/A=200$ MeV (upper panels). The lines represent calculations based on single-particle emission probabilities [cf. Eq. (7)].

Here, $\Pi_1(\mathbf{p}_1)$ denotes the one-particle probability obtained by integrating the two-particle emission probability over the impact parameter $\mathbf{b}$, all emission points $\mathbf{r}_1$ and $\mathbf{r}_2$, and the momenta $\mathbf{p}_2$ of one of the protons, i.e.,

$$\Pi_1(\mathbf{p}_1) = \int d\mathbf{b}\, d\mathbf{p}_2 d\mathbf{r}_1 d\mathbf{r}_2 \Pi_2(\mathbf{p}_1,\mathbf{p}_2,\mathbf{r}_1,\mathbf{r}_2)\hat{C}(\mathbf{q},\mathbf{r}_1-\mathbf{r}_2)\delta(|\mathbf{p}_1-\mathbf{p}_2'|-q)\,. \tag{5}$$

Because of the limited statistics in microscopic simulations a finite integration window Δ is required in computing the theoretical CFs. This is achieved by introducing a step function $\Theta_\Delta(q)$ which is 1 for relative momenta $|\mathbf{p}_1-\mathbf{p}_2| - \Delta \le q \le |\mathbf{p}_1-\mathbf{p}_2| + \Delta$ and 0 otherwise [16]. The corresponding correction factor reads

$$C_\Delta(q) = \frac{\int d\mathbf{b}\, d\mathbf{p}_1 d\mathbf{p}_2 d\mathbf{r}_1 d\mathbf{r}_2 \Pi_2(\mathbf{p}_1,\mathbf{p}_2,\mathbf{r}_1,\mathbf{r}_2)\hat{C}(\mathbf{q},\mathbf{r}_1-\mathbf{r}_2)\delta(|\mathbf{p}_1-\mathbf{p}_2|-q)}{\int d\mathbf{b}\, d\mathbf{p}_1 d\mathbf{p}_2 d\mathbf{r}_1 d\mathbf{r}_2 \Pi_2(\mathbf{p}_1,\mathbf{p}_2,\mathbf{r}_1,\mathbf{r}_2)\hat{C}(\mathbf{q},\mathbf{r}_1-\mathbf{r}_2)\Theta_\Delta(q)} \frac{\int d\mathbf{p}_1 d\mathbf{p}_2' \Pi_1(\mathbf{p}_2')\Pi_1(\mathbf{p}_1)\Theta_\Delta(q)}{\int d\mathbf{p}_1 d\mathbf{p}_2' \Pi_1(\mathbf{p}_2')\Pi_1(\mathbf{p}_1)\delta(|\mathbf{p}_1-\mathbf{p}_2'|-q)}\,. \tag{6}$$

Assuming an independent emission of the two protons, and neglecting $C_{\rm dyn}(q)$ as well as $C_\Delta(q)$, the CF can be expressed in accordance with Ref. [15] in terms of the one-particle source function $\Pi_1(\mathbf{p},\mathbf{r})$:

$$R(q)+1 = \frac{\int d\mathbf{b}\, d\mathbf{p}_1 d\mathbf{p}_2 d\mathbf{r}_1 d\mathbf{r}_2 \Pi_1(\mathbf{p}_1,\mathbf{r}_1)\Pi_1(\mathbf{p}_2,\mathbf{r}_2)\hat{C}(\mathbf{q},\mathbf{r}_1-\mathbf{r}_2)\Theta_\Delta(q)}{\int d\mathbf{b}\, d\mathbf{p}_1 d\mathbf{p}_2 d\mathbf{r}_1 d\mathbf{r}_2 \Pi_1(\mathbf{p}_1,\mathbf{r}_1)\Pi_1(\mathbf{p}_2,\mathbf{r}_2)\Theta_\Delta(q)}\,. \tag{7}$$

In the BUU [17] and QMD [18] calculations nucleons were considered to be emitted when the surrounding density fell below a value ρ_e before the time $t_f = 150$ and 200 fm/c, respectively. Whereas for the BUU events this was the only selection criterion to evaluate the single-particle emission probability, we consider two cases in the QMD simulations:

(1) Comparable to the BUU calculations only unbound protons for which no other nucleon exists within a coalescence radius of $r_f = 3$ fm [19] at t_f were considered for evaluating the *single*-particle emission probability $\Pi_1(\mathbf{p},\mathbf{r})$.

(2) The *two*-particle emission probability $\Pi_2(\mathbf{p}_1,\mathbf{p}_2,\mathbf{r}_1,\mathbf{r}_2)$ is dominated by pairs of two unbound protons which are, however, from the same event. In addition, Π_2 includes all diproton clusters giving rise to a more pronounced peak at $q \approx 20$ MeV/c. Furthermore, all proton pairs are taken into account where either one is bound in a diproton and the other one is free or both are bound in two different diprotons.

Results of calculations employing Eq. (7)—i.e., probing the FSI essentially with two protons from *different* events—are summarized in Fig. 2. Figures 2(a) and 2(b) display the predictions based on BUU simulations. The solid and dashed lines correspond to calculations using a soft (compressibility $K = 200$ MeV) and a stiff ($K = 380$ MeV) equation of state (EOS), respectively. The emission density ρ_e was assumed to be $\frac{1}{8}$ of normal nuclear density ρ_0. Consistent with previous studies at intermediate energies [15] the calculations exploiting a stiff EOS reproduce the observed energy dependence rather well for the $E/A = 60$ MeV reaction [Fig. 2(b)]. A similar energy dependence is also found with a soft EOS although the magnitude of the correlation is overpredicted. However, at $E/A = 200$ MeV the calculated average CFs $\langle R(q)+1\rangle_{15-27}$ show for the soft as well as for the stiff EOS a pronounced dependence on the summed energy which is clearly inconsistent with the data [Fig. 2(a); the corresponding CFs for a soft EOS are shown by the dashed histograms in Fig. 1].

Calculations based on single-particle emission probabilities predicted by QMD simulations are displayed in Figs. 2(c)–2(f). For a soft EOS with a nuclear compressibility constant $K = 200$ MeV, the QMD predictions are at both energies rather similar to the corresponding BUU results shown in Figs. 2(a) and 2(b). At $E/A = 60$ MeV [Fig. 2(d)] the total increase of the correlation with increasing $E_{\rm sum}$ corresponds reasonably well to the experimentally observed rise. Using a soft EOS with momentum-dependent interaction (MDI) does not improve the agreement between the experimental observations at $E/A = 200$ MeV [dashed line in Fig. 2(c)].

Because of the stronger localization in coordinate space at higher emission density ρ_e the correlation increases with increasing ρ_e [Figs. 2(e) and 2(f)]. Nonetheless, in view of the weak sensitivity to ρ_e the deviation from the data at $E/A = 200$ MeV could only be reduced significantly by using an unreasonably low emission density possibly indicating the importance of density fluctuations.

From the preceding discussion it appears that calculations based on single-particle phase space distributions which ignore any correlation within an event prior to the emission cannot reproduce the CFs for the ^{40}Ar+^{197}Au reaction at $E/A = 200$ MeV. In a further attempt to resolve this discrepancy we generated the CFs on the basis of two-particle emission probabilities predicted by the QMD model. For our experimental conditions and within the statistical uncertainties of typically 10% the product $C_{\rm dyn}(q)C_\Delta(q)$ turns out to be rather flat for $q < 120$ MeV/c and increases only slowly for larger q. In the following we, therefore, assume $C_{\rm dyn}(q)C_\Delta(q)$ to be constant and show in Fig. 3 the results of calculations based on Eq. (3) only. For all calculated values displayed in Fig. 3 the statistical uncertainties are less than 5%. Simulations using an emission density $\rho_e = \frac{1}{4}\rho_0$ are still inconsistent with the data at $E/A = 200$ MeV (dashed line in Fig. 3 top). However, the CFs are rather well reproduced if $\rho_e = \frac{1}{8}\rho_0$ is chosen (solid line). The strong ρ_e dependence reflects the spatial separation of the two

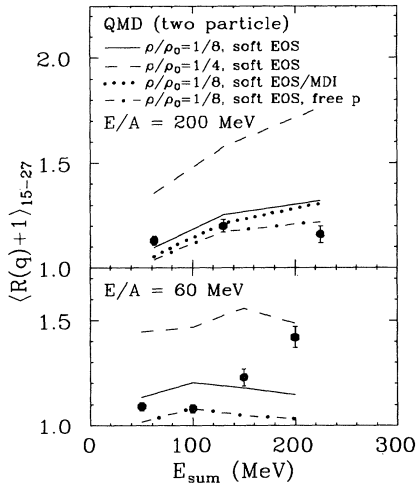

FIG. 3. Average height $\langle R(q)+1\rangle_{15\text{-}27}$ of the two-proton correlation functions as a function of the sum energy E_{sum} for $^{40}\text{Ar}+^{197}\text{Au}$ reactions at $E/A=60$ MeV (lower part [6]) and $E/A=200$ MeV (upper part). The lines represent calculations based on two-particle emission probabilities [cf. Eq. (3)] predicted by QMD simulations.

protons due to their repulsive interaction and/or the influence of adjacent clusters. Combining protons from two different events disregards this mutual interaction during the emission and, thus, weakens the ρ_e dependence [Figs. 2(e) and 2(f)]. In contrast to ρ_e, the momentum dependence of the interaction seems to not exert a significant influence (see dotted line).

In order to investigate the role of diproton clusters we evaluated $R(q)$ for those events where both protons are free (dash-dotted curves in Fig. 3). For all kinetic energies, $\langle R(q)+1\rangle_{15\text{-}27}$ is below the values of the corresponding full calculations (solid lines). Thus, the reduction of the CF at $E/A=200$ MeV originates mainly from correlations prior to the emission of unbound protons whereas diprotons cause only a minor correction.

The CFs for a soft EOS and $\rho_e=\rho_0/8$ are shown by the solid histograms in Fig. 1. Although these calculations include the effects of diprotons, there is still a remarkable difference between the data and the calculations at relative momenta $q<10$ MeV/c. Partially this enhanced coincidence yield at very small relative momenta can be attributed to emission processes during later stages of the reaction [6,20]. These sequential processes will not only increase the calculated CF at very small relative momenta $q\leq 10$ MeV/c, but will also decrease the maximum at $q\approx 20$ MeV/c. Whereas the agreement for the 200 MeV data at large E_{sum} and the 60 MeV data at small E_{sum} will be improved, the 200 MeV data at small kinetic energies will be slightly underpredicted. The most significant deviation persists, however, for the most energetic protons at $E/A=60$ (bottom part of Fig. 3). One might speculate whether additional intrinsic two- or higher-body quantum correlations which are not yet taken into account in the QMD model are relevant for the formation of these proton pairs with velocities far beyond the beam velocity.

In conclusion, the present analysis clearly indicates that two-particle correlation functions are strongly effected by "true" correlations between the individual nucleons within a single event. This raises the hope that future studies of two-particle correlations may provide important information about the size of fluctuations and the development of instabilities in highly excited nuclear systems.

The authors thank W. Bauer and J. Aichelin for the use of the BUU and QMD code, respectively, and for helpful discussions. One of us (J.P.) acknowledges the financial support of the Deutsche Forschungsgemeinschaft.

[1] S. E. Koonin, Phys. Lett. **70B**, 43 (1977).
[2] F. Zarbakhsh *et al.*, Phys. Rev. Lett. **46**, 1268 (1981).
[3] W. G. Lynch *et al.*, Phys. Rev. Lett. **51**, 1850 (1983).
[4] H. A. Gustafsson *et al.*, Phys. Rev. Lett. **53**, 544 (1984).
[5] J. Pochodzalla *et al.*, Phys. Lett. B **174**, 36 (1986).
[6] J. Pochodzalla *et al.*, Phys. Rev. C **35**, 1695 (1987).
[7] T. C. Awes *et al.*, Phys. Rev. Lett. **61**, 2665 (1988).
[8] P. Dupieux *et al.*, Z. Phys. A **340**, 165 (1991).
[9] S. Pratt and M. B. Tsang, Phys. Rev. C **36**, 2390 (1987).
[10] S. E. Koonin, W. Bauer, and A. Schäfer, Phys. Rev. Lett. **62**, 1247 (1989).
[11] J. Pochodzalla *et al.*, Phys. Lett. B **175**, 275 (1986).
[12] F. Zhu *et al.*, Phys. Rev. C **44**, R582 (1991).
[13] S. Yu. Kun, R. Gentner, and L. Lassen, Z. Phys. A **342**, 67 (1992).
[14] S. Pratt and W. Bauer, in *Proceedings of CORINNE 90, International Workshop on Particle Correlations and Interferometry,* edited by D. Ardouin (World Scientific, Singapore, 1990), p. 183.
[15] W. G. Gong *et al.*, Phys. Rev. Lett. **65**, 2114 (1990); Phys. Rev. C **43**, 781 (1991).
[16] In the QMD simulations a value of $\Delta=100$ MeV/c was adopted whereas in the BUU simulations on each individual component of the calculated relative momentum vector a gate of 20 MeV/c was applied. The latter corresponds to the default value given in the program which was employed in Ref. [15] [W. Bauer (private communication)]. Using for the QMD calculations $\Delta=50$ MeV/c did not change the results notably.
[17] W. Bauer (private communication); the present calculations were performed with 100 test particles and the free nucleon-nucleon cross sections.
[18] J. Aichelin and H. Stöcker, Phys. Lett. B **176**, 14 (1986); for a recent review see J. Aichelin, Phys. Rep. **202**, 233 (1991).
[19] Changing the coalescence radius by ± 1 fm modified the results presented in Figs. 2 and 3 by less than $\pm 5\%$.
[20] G. J. Kunde *et al.*, Phys. Lett. B **272**, 202 (1991).